90-GHz Band Propagation Characteristics in Viaduct Environment for Railway Radiocommunication System Between Train and Trackside

Hirokazu Sawada[1], Kentaro Ishizu[1], Fumihide Kojima[1], Hiroyo Ogawa[1], Kazuki Nakamura[2], Nagateru Iwasawa[2], Kunihiro Kawasaki[2], Nobuhiko Shibagaki[3]
1 National Institute of Information and Communications Technology, Yokosuka, Japan
2 Railway Technical Research Institute, Kokubunji, Japan
3 Hitachi Kokusai Electric Inc., Kodaira, Japan
sawahiro@nict.go.jp

***Abstract*— For railway radio communication systems between train and trackside, utilization of the 90 GHz band is considered in Japan. To design the system and evaluate the interference to other radio systems, propagation characteristics should be clarified for various usage environments. In this paper, propagation characteristics of path loss and r.m.s. delay spread are described based on measurement results in a viaduct environment. Path loss coefficients are extracted at different antenna heights compared with the side wall height of viaduct for a link budget design and it is validated by ray trace simulation. The cumulative distribution of delay spread is also analyzed for physical layer design. The system parameter of railway communication system in 90 GHz band is suggested by considering these propagation characteristics.**

Keywords*— millimeter-wave, railway communication, path loss, r.m.s. delay spread

I. INTRODUCTION

In the current railway radio system between train and trackside in Japan, the leaky coaxial cable communication system [1, 2] is used for high speed railway transportation, and its throughput is limited to a few Mbps by the signal bandwidth in 400 MHz band. For the future railway system, the throughput improvement is required for transmitting sensing/traffic control signals and high resolution video surveillance in the train for safety operation. For these purposes a broadband railway radio communication system using millimeter-wave is considered in Japan [3, 4].

Millimeter-wave band railway radio communication system was studied since the 1980's in Japan. Utilization of the 40 GHz and 50 GHz band were considered in the previous developments [5, 6] and recently 90 GHz band [7] is also considered as a candidate which has wider bandwidth. Therefore the study of propagation characteristics and device prototyping are on-going to develop the 90 GHz band railway communication system.

Propagation characteristics in the open-space railway environment [8] and the loss of rain and snow were reported [9, 10] by the recent studies. In this study, propagation characteristics of path loss and r.m.s. delay spread in the viaduct environment are analyzed as another environment. Path loss coefficients are extracted at different antenna heights compared with the side wall height of viaduct. The measured path loss results are validated by ray trace simulation with considering multiple reflection waves in the viaduct structure. Power delay profiles along the viaduct course are also measured, and r.m.s. delay spreads are analyzed by its cumulative distribution.

The paper organization is as follows. Section II discusses the propagation measurement of path loss and delay spread. The ray trace simulation is described in Sections III to validate the measured path loss characteristics. Section IV gives the conclusions.

II. PROPAGATION MEASUREMENT IN VIADUCT ENVIRONMENT

A. Measurement Environment and Parameters

In the railway radio communication system, viaduct is one of the usage environments. Viaduct is the long bridge made of multiple small spans. In this study the viaduct has side walls along a railway track as shown in the Fig. 1, because the viaduct was used as the test course for a maglev train in Miyazaki, Japan. Figure 2 shows the snapshot of the measurement in the viaduct environment. The cross-sectional size of viaduct is 3.45 m width and 1.24 m height as shown in Fig. 3. For millimeter wave railway communication systems, it is considered as a suitable plan to form the communication area along a railway track by using a high gain antenna. For path loss measurement, the horn antennas of 25 / 20.3 dBi gain, which is changed by polarization of vertical and circular, were used for transmitter (TX) and receiver (RX). RX was fixed and TX was moved by using a trailer to measure a distance dependence. TX and RX antenna positions were set in the center of viaduct and its heights were set at 1 or 2 meters of same heights above the viaduct floor as shown in Fig. 2. The antenna heights were set as high or low positions compared to the sidewall height of viaduct. The maximum transmission distance was 500 meters in the line-of-sight situation because the output power has limitation by a used RF device performance. The measured polarization was set to vertical or circular (left hand) to study the polarization difference. The

978-1-5386-2768-6/17/$31.00 ©2017 IEEE

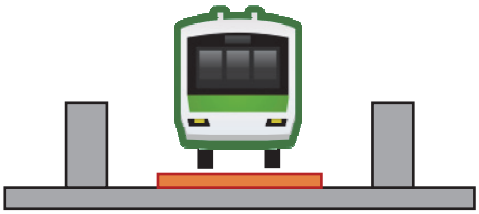

Fig. 1. Viaduct environment in this study

Fig. 2. Snapshot of measurement in the viaduct

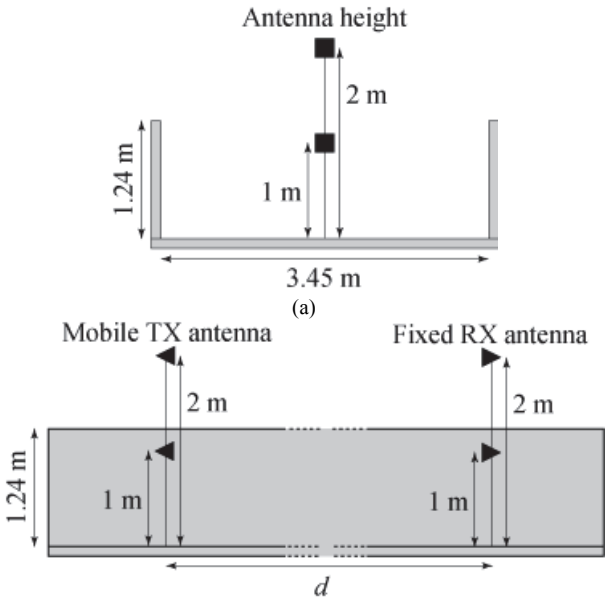

Fig. 3. Viaduct structure and antenna position. (a) Cross sectional view (b) Side view.

TABLE I. MEASUREMENT PARAMETER

Parameter	Value
Center frequency	93.56 GHz
Signal band width	2.16 GHz
Antenna gain of TX and RX	25 dBi (Vertical Pol.) 20.3 dBi (Circular Pol.)
Antenna height	1, 2 m
Polarization	Vertical, Circular (LH)
Distance	10 - 500 m

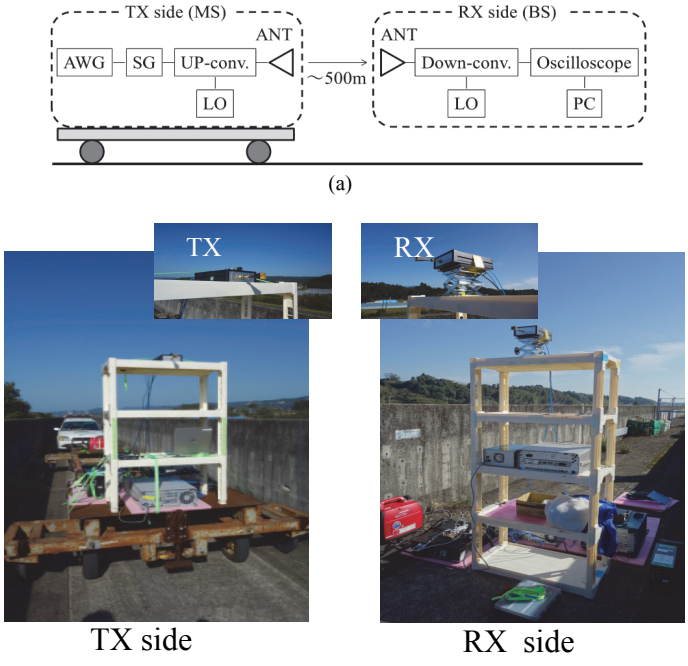

Fig. 4. Measurement system (a) TX and RX configurations (b) Snapshots of TX and RX.

power spectrum and delay profiles were measured by using an OFDM signal. The center frequency of the signal was 93.56 GHz and the frequency bandwidth was 2.16 GHz. Table 1 summarizes these parameters.

Figure 4 shows the measurement system for the viaduct environment. In the TX side, the IQ signals generated by an arbitrary waveform generator (AWG) are input to the signal generator to make a modulated inter-frequency (IF) signal. The IF signal is up-converted to the radio frequency (RF) signals in 90 GHz band. In the RX side, the received signal is down-converted, and captured by an oscilloscope. The captured signals are analyzed by a computer to obtain the path loss and power delay profiles. The snapshots of transmitter and receiver are shown in the Fig. 4b.

B. Path Loss Measuremrnt in the Viaduct Environment

Figure 5 shows the measured path loss for different antenna height when both antenna polarizations were set to vertical. To develop the path loss model, the following equations are adopted to extract a path loss coefficient.

$$PL = L_0 + 10n \log_{10}(d / d_0) \quad (1)$$

$$L_0 = 20 \log_{10} f_0 - 28 \quad (2)$$

Where, f_0 (MHz) is the center frequency of signal, n is the path loss coefficient, and d and d_0 are distance and the reference distance.

By a linear approximation approach to measured results, path loss coefficients were extracted as n = 1.52 and 1.13 for 2

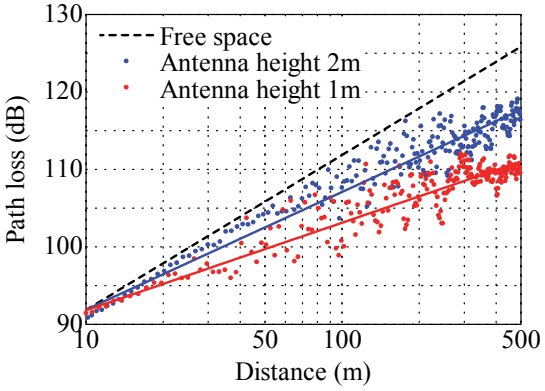

Fig. 5. Path loss characteristics for different antenna heights

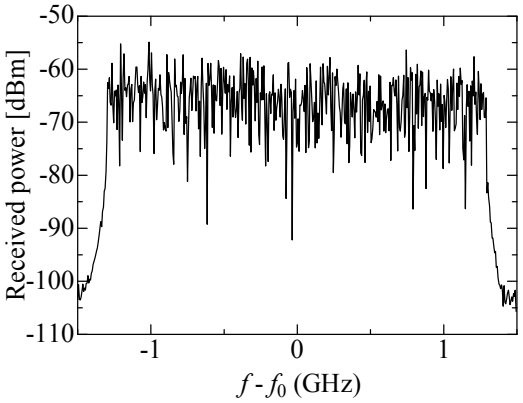

Fig. 7. Example of measured frequency spectrum

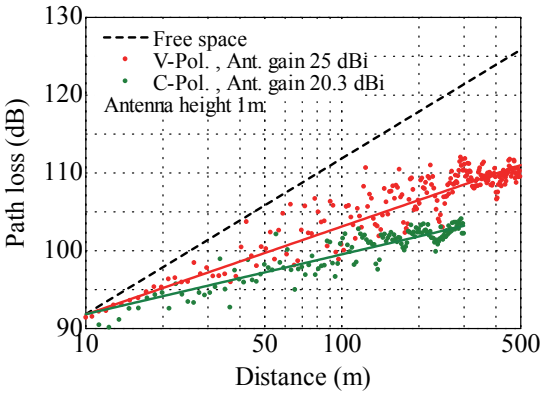

Fig. 6. Path loss characteristics for different polarizations

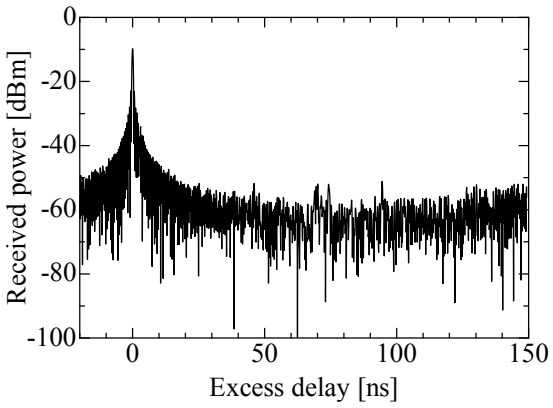

Fig. 8. Example of measured power delay profile

and 1 m antenna heights, respectively. In the approximation process, the reference distance is set to 10 m. Extracted pass loss coefficients were smaller than it of the free-space path loss (n = 2) and it became smaller when antenna height was lower. It is considered as a similar phenomenon in a street canyon environment of mobile cellular communication, because the propagation path is surrounded by floor and sidewall of the viaduct. The reason of the low path loss coefficients is examined by ray trace method analysis in the Section III.

For the polarization difference, the circular polarized signal was also used when the antenna height was 1 m. The measured path loss for circular polarized signal is shown in figure 6 with the measured data of the vertical signal for comparison. The extracted path loss coefficient for circular polarized signal was n = 0.77, and it was much lower than it of vertical polarization. This is possibly caused by the gain difference of used antenna. Since the antenna beam width has some difference for two polarization signals, the power of reflection wave from sidewall was increased by using wider antenna beam, and it is considered that the path loss was decreased.

C. Delay Spread Measuremrnt in the Viaduct Environment

Frequency responses were measured by using demodulated IQ signals of each OFDM sub-carrier. Figure 7 is an example of the measured frequency response. Therefore, the impulse response is calculated by Fourier transformation of the frequency response, and the power delay profile is calculated by averaging the four impulse responses in this processing. Figure 8 is an example of calculated power delay profile.

As an evaluation method of power delay profiles, a statistic analysis of the r.m.s. delayed spread is generally used for designing the system. The delay spread is calculated by using the following equation.

$$\sigma = \sqrt{\frac{\sum_{i=1}^{N} P_i \tau_i^2}{\sum_{i=1}^{N} P_i} - \frac{\left(\sum_{i=1}^{N} P_i \tau_i\right)^2}{\left(\sum_{i=1}^{N} P_i\right)^2}} \qquad (3)$$

where P_i and τ_i are the power and relative delay time of i-th data of the measured power delay profile. To calculate the delay spread without noise signal, a threshold level is required generally. In this paper the delay waves, which are from peak power to the 20 dB lower level in the power delay profile, are included in the calculation of the delay spread. The delay

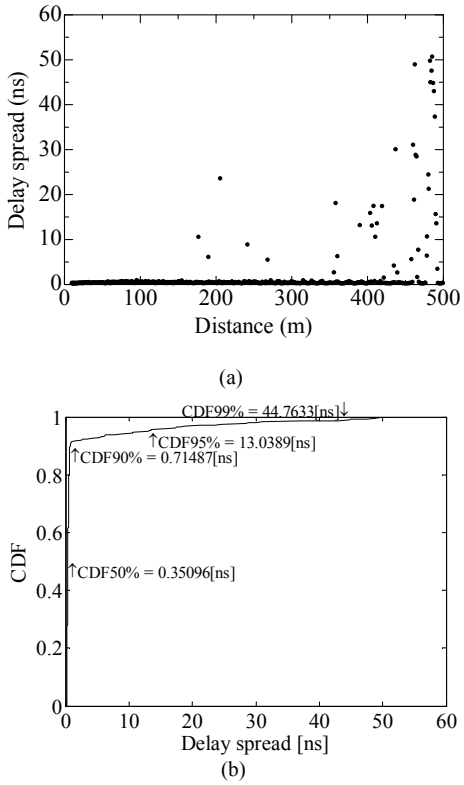

Fig. 9. Delay spread results (Antenna heights are 2 m, V-pol.) (a) Distribution for the measured distance (b) CDF

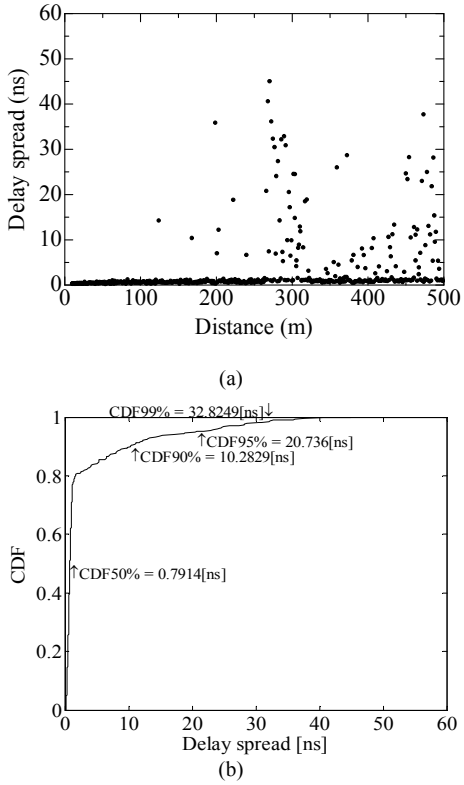

Fig. 10. Delay spread results (Antenna heights are 1 m, V-pol.) (a) Distribution for the measured distance (b) CDF

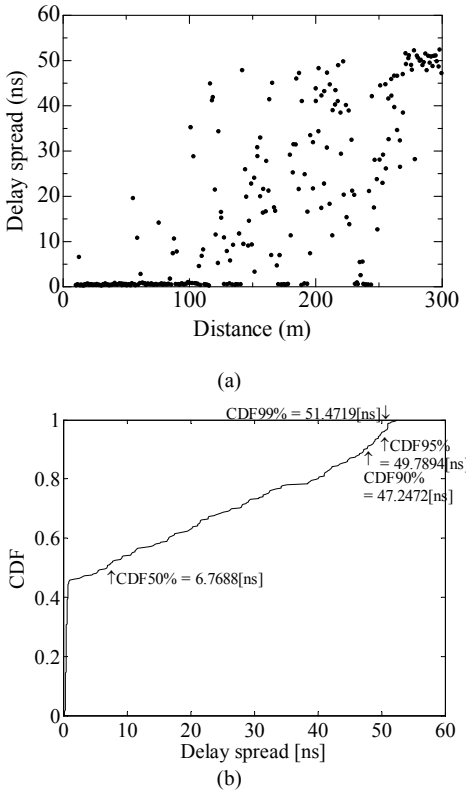

Fig. 11. Delay spread results (Antenna heights are 1 m, C-pol.(LH)) (a) Distribution for the measured distance (b) CDF

spread values at each measured position along the viaduct are plotted in the Fig. 9a when the antenna height was 2 m and vertical polarized signal was used. The delayed spread beyond 1 ns was not observed in the short distance up to 150 m. The delay spread exceeding 1 ns was sometimes observed in the middle distance from 150 to 400 m. In the long distance over 400 m, the maximum delay spread was increased up to 50 ns. This means the number of delayed waves by multiple reflections are increased in the long distance. A cumulative distribution function of the delayed spread of figure 9a is represented in figure 9b. The delay spread is 0.35 ns at CDF=50%, 0.71 ns at CDF=90% and 13 ns at CDF=99%. It is also investigated the delay spread could be decreased to 8.8 ns at CDF=99% if the communication range is assumed as 400 m. Thus the relationship of delay spread and distance provides a consideration for the modulation and coding scheme.

Figure 10 shows the delay spread values at the measured distance and its distribution when the antenna height was 1 m and vertical polarized signal was used. From these results, the delay spread at CDF=50% was 0.79 ns which is doubled value of when the antenna height was 2 m. The delay spread increased to around 10 ns at CDF=90% and it has an influence for the system design. These results agree with the path loss of Fig. 5. The path loss was decreased by increasing the number of delay waves. Low path loss is an advantage for link budget, however, the large delay spread causes a complexity for physical layer design.

TABLE II. PATH LOSS COEFFICIENTS AND ANALYSIS RESULTS OF R.M.S. DELAY SPREAD DISTRIBUTION

Ant. HPBW (deg.)		Ant. Height (m)	Pol.	Path loss n	CDF of Delay Spread (ns)	
TX	RX				50%	95%
10	10	2	V	1.52	0.35	13
10	10	1	V	1.13	0.79	21
15	15	1	C	0.77	6.76	50

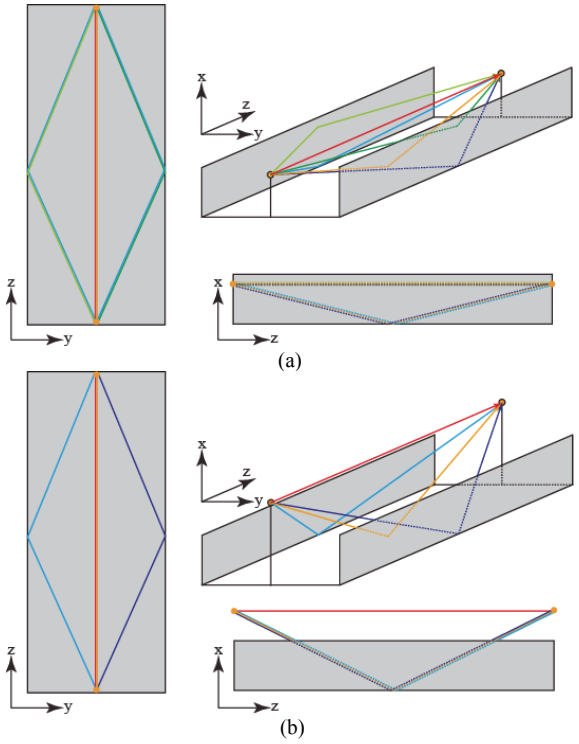

Fig. 12. Direct and one-time reflection waves calculated in ray-tracing simulation (a) Antenna heights are 1 m (b) Antenna heights are 2 m

Figure 11 is shown for circular polarized signal when the antenna height was 1 m. The delay spread was larger than when the vertical polarized signal was used. It was large of 6.8 ns even at the CDF=50%. This result also corresponds to the low path loss characteristics as shown in Fig. 6. The extracted parameters of path loss coefficients and delay spread distributions are summarized in Table II.

III. PATH LOSS ANALYSIS BY RAYTRACE METHOD

In this section, measured path loss coefficients are validated by ray-tracing simulation. For modelling the viaduct environment as shown in Fig. 3. Viaduct structure is simplified as three concreate plates. By changing both antenna heights of transmitter (TX) and receiver (RX), the number of reflection path is changed. Figure 12 shows the examples of ray-tracing paths for direct and one-time reflection waves, and Figure 13 also shows the path for two- and three-time reflection waves. For more reflection wave paths also

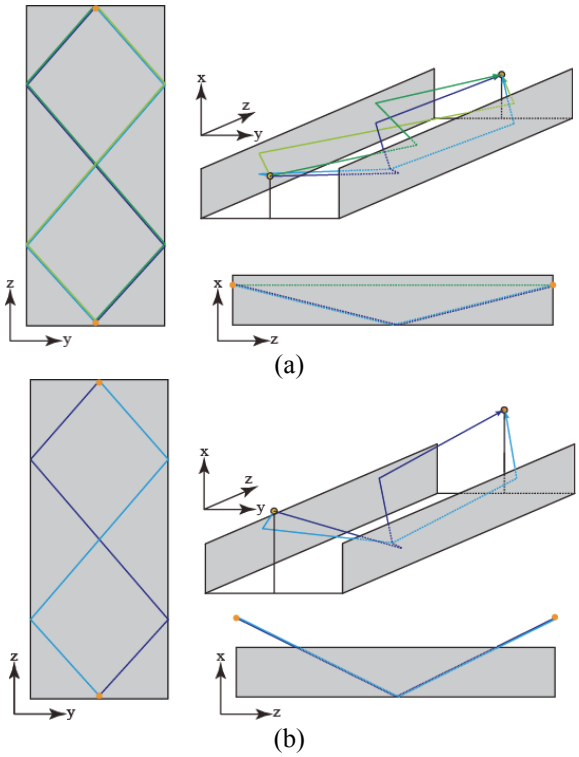

Fig. 13. Two-time reflection waves calculated in ray-tracing simulation (a) Antenna heights are 1 m (b) Antenna heights are 2 m

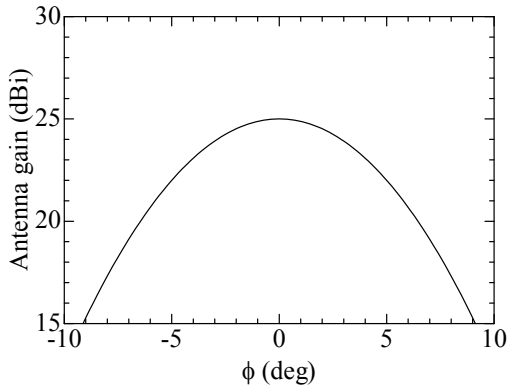

Fig. 14. Antenna gain model in ray-tracing simulation

calculated in the same manner. Diffraction waves are not considered in the simulation, since these power is much smaller than reflection waves.

The parameters of Table I are used in the simulation. To simulate ray-tracing, the antenna main beam directivity and gain is modelled by assuming a quadratic function as follows.

$$G = G_0 - \alpha\phi^2 \quad (4)$$

where, G_0 = 25 (dBi) and α = 0.12 for HPBW=10 (degree). ϕ (degree) is the angle in both vertical and horizontal. Figure 14 shows the main beam gain function of antenna model.

For the ray-tracing simulation in multipath rich environment, the number of paths are important. Enough

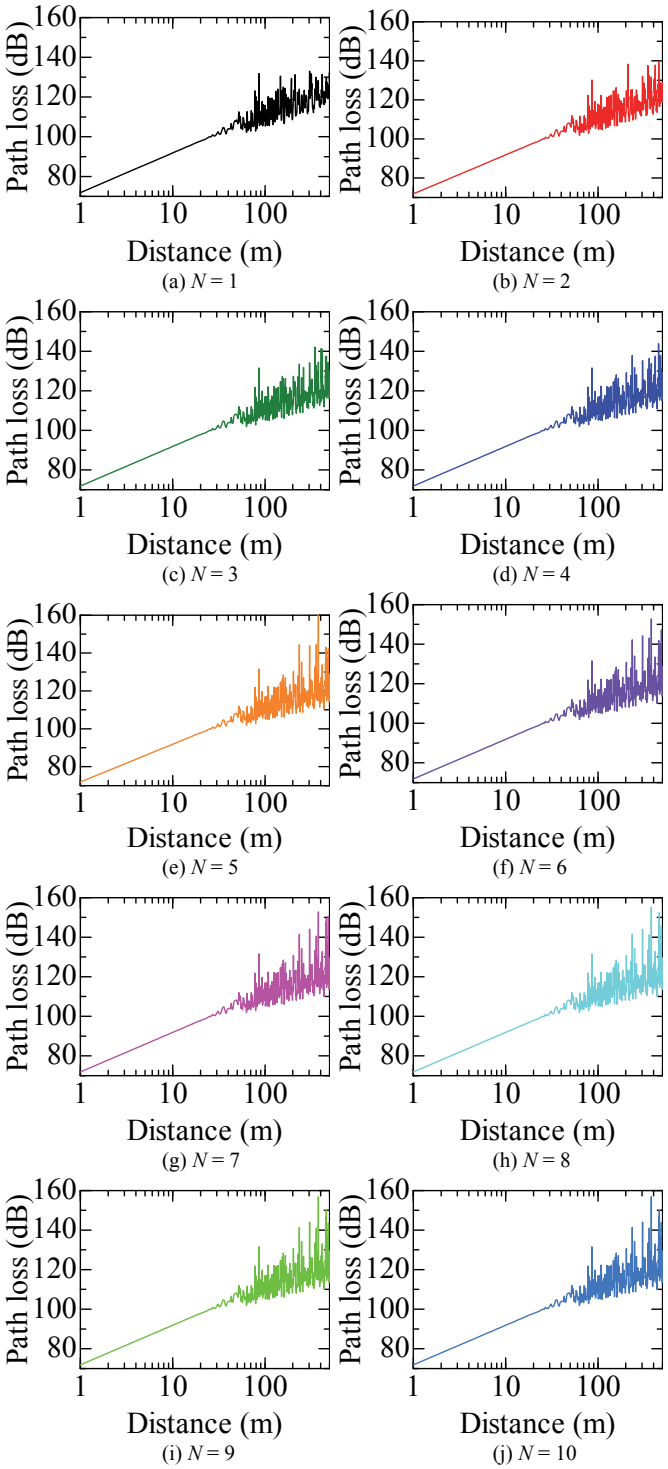

Fig. 15. Simulated path loss when reflection number (N) is changed

number of paths is confirmed by increasing the number of reflection in the ray tracing simulation. Simulated results are compared as shown in Fig. 15 while reflection number (N) is increasing from 1 to 10. Figure 16 shows the maximum error in 1 m step path loss between the results in N times reflection and N - 1 times reflection conditions when the antenna height is 2 m. From this figure, the error becomes less than 1 dB when the number of reflection is 10, and the maximum

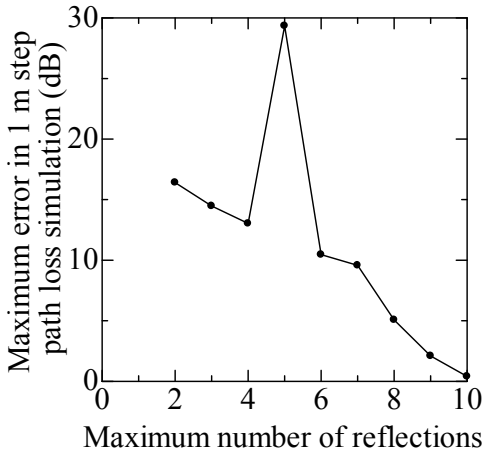

Fig. 16. Maximum error in 1 m step path loss simulation when reflection number (N) is changed

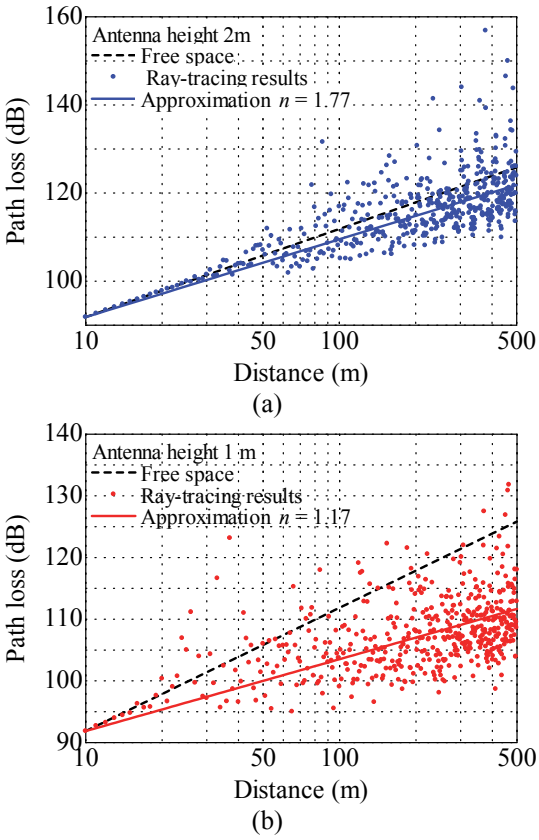

Fig. 17. Simulated path loss results (Antenna heights are 1 and 2 m, V-pol.)

reflection number is set to N = 10.

Figure 17 shows simulation results of path loss characteristics when antenna heights are 1 and 2 m. From these ray tracing simulations, path loss coefficients are extracted as n = 1.17 and 1.77 for each antenna height is 1 and 2 m. On the other hand, path loss coefficients of measured path loss are extracted as n = 1.13 and 1.52 for each antenna height of 1 and 2 m by setting the reference distance is 10 m. Both simulation and measured coefficients are less than n = 2 of the free space loss, and it is confirmed that the coefficient become smaller when the antenna height is lower.

978-1-5386-2768-6/17/$31.00 ©2017 IEEE

IV. Conclusion

The 90 GHz band propagation characteristics in the viaduct environment were examined by measurement and simulation results. The path loss coefficient were smaller than the free space (n = 2) and became more smaller when the antenna height was lower. This small path loss coefficient affected to the delay spread which verified in the cumulative distribution analysis. To examine the lowest path loss when the circular polarized signal was used is future work.
These extracted propagation parameters in the viaduct environment will give a consideration for designing the millimeter-wave railway communication system.

Acknowledgment

This research was conducted under a contract of R&D for radio resource enhancement, organized by the Ministry of Internal Affairs and Communications, Japan.

References

[1] K. Mikoshiba and Y. Nurita, “Guided radiation by coaxial cable for train wireless systems in tunnels,” IEEE Trans. Veh. Technol., vol. 18, no. 2, pp. 66–69, Aug. 1969.

[2] T.Yuge and S.Sasaki, "Train radio system using leaky coaxial cable," Proc. of 34th IEEE Vehicular Technology Conference, pp.43-48, 1984.

[3] K. Tsukamoro, Y. Kato, S. Umeda, N. Kawahara, H. Nagayama, K. Kawasaki, K. Nakamura, H. Tsuji, A. Okazaki, F. Ishizu, "Field-Test Results of Mobile Communication Systems over 40 GHz Frequency Band," Proc. of 11th IEEE Vehicular Technology Society Asia Pacific Wireless Communications Symposium, 2014.

[4] T. Hattori, R. Nakamura, A. Kurita, H. Kimura, "Study of a Millimeter Wave Communications System for Railway Trains," JR East Technical Review, No.33, pp.37-42, 2015.

[5] H. Meinel, A. Plattner, G. Reinhold, "A 40 GHz Railway Communication System," IEEE Journal on Selected Areas in Communications, vol.1, no.4, Sep. 1983.

[6] H. Yamamura, S. Sasaki, "Millimeter Wave Propagation Model and Delay Spread along the Maglev Guideway," IEICE Trans., Vol.E78-B, no.8, pp. 1204-1207, Aug. 1995.

[7] K. Nakamura, K. Kawasaki, N. Iwasawa and D. Yamaguchi, "Application of the 90GHz Band Millimeter-Wave in the Railway," Proc. of 11th World Congress on Railway Research, 2016.

[8] K. Nakamura, K. Kawasaki, K. Takeuchi, N. Yonemoto, A. Kohmura, S. Futatsumori, “Radio Propagation Characteristics of the 90 GHz Millimeter-Wave in Railway Environment,” IEICE Tech. Rep., vol. 113, no. 333, MWP2013-53, pp. 33-38, Nov. 2013 (in Japanese).

[9] K. Nakamura, K. Kawasaki, N. Iwasawa, D. Yamaguchi, K. Takeuchi," The Monitoring System Using 90GHz Band for Railway," Proc. of the International Symposium on Speed-up and Sustainable Technology for Railway and Maglev Systems, 2015.

[10] K. Nakamura, N. Iwasawa, K. Kawasaki, " The Attenuation Characteristics of 90GHz Band Millimeter Wave by Snow," Proc. of the IEICE General Conference, B-1-19, p.19, 2016 (in Japanese).